

Debonding Identification of FRP Strengthened Concrete Beams with PZT Sensors

Ricardo PERERA¹, Rui SUN¹, Enrique SEVILLANO¹, Marta BAENA², Cristina BARRIS²

¹ Dpt Mechanical Engineering, Technical University of Madrid, José Gutiérrez Abascal 2, 28006 Madrid (Spain) perera@etsii.upm.es

² Analysis and Advanced Materials for Structural Design (AMADE), Polytechnic School, University of Girona, Campus Montilivi s/n, 17071 Girona, Spain

Key words: FRP strengthening; Concrete; Debonding; Electromechanical impedance; Spectral model; Structural health monitoring.

Abstract

In the present work, debonding detection in RC beams externally flexural strengthened with FRP composites using the EMI technique is explored. For this, a model updating procedure will be developed. To make the proposed methodology successful one of the main objectives is the implementation of a bonded-PZT-FRP spectral beam element to be used in the calculation of the electrical admittance of the PZT transducers bonded to the structure. The use of the finite element method in a high frequency SHM approach, such as impedance-based method, would require a high number of elements of small size with an enormous expense in computation time and effort since the element size has to be comparable to wavelengths, which are very small in high frequencies. One of the advantages of the formulation presented here, based on the spectral element method (SEM), is its accuracy to provide solutions in the high frequency range. Therefore, this approach in conjunction with the use of PZT actuator-sensors mounted on the structure might be used for a more reliable debonding detection between an FRP strip and the host RC structure. The updating procedure is solved by using an ensemble particle swarm optimization (PSO)-based approach

1 INTRODUCTION

Nowadays, fiber reinforced polymers (FRP) have found widespread usage in civil structures, especially for the strengthening and rehabilitation of existing concrete structures [1, 2, 3]. High strength-to-weight ratio, resistance to corrosion, and ease of handling are among the main advantages of FRP composites. However, considering that structures are often subjected to unexpected loading and severe environmental conditions over their life cycle, structural damage and deterioration might also appear in strengthened structures. Unfortunately, strengthening with FRP is often associated with a brittle and sudden failure caused mainly by some form of debonding of the FRP from the concrete. As reported in the literature, the primary causes for such abrupt failure are the stress concentration at the FRP strip cutoff point, which might cause plate end debonding [4, 5], and in the vicinity of transverse cracks along the beam span, which would originate an intermediate crack debonding [6, 7, 8]. This latter debonding mode is considered to be a more dominant failure



mode compared to plate end debonding, especially for thin FRP plates. To avoid this failure mode and their catastrophic consequences, the implementation of a method for field monitoring of repaired members would be suitable, since local debonding is not detectable from a simple visual observation.

Structural health monitoring systems have been proposed for this purpose based on strain tracking. One of the main disadvantages of this approach is due to the need to use expensive finite element models to carry out the procedure, able to define the stage of the concrete/composite bond from the measured strain distribution. However, although some attempts have been made recently to eliminate this shortcoming [9], detection techniques based on strains are also restrained by their limited sensitivity to identify minor defects such as those that might originate the debonding failure. Furthermore, the use of controlled load tests or monitoring the traffic while the structure is in operation to obtain suitable strain profiles increase the complexity of the damage identification procedure.

In the present work, a methodology of debonding detection in concrete beams externally flexural strengthened with FRP composites using the electro-mechanical impedance technique is explored. For this, a model updating procedure will be developed. To make the proposed methodology successful one of the main objectives is the implementation of a bonded-PZT-FRP spectral beam element to be used in the calculation of the electrical admittance of the PZT transducers bonded to the structure. Spectral element method (SEM) provides accurate solutions in the high frequency range. Therefore, this approach in conjunction with the use of PZT actuator-sensors mounted on the structure might be used for a more reliable debonding detection between an FRP strip and the host concrete structure.

2 SPECTRAL MODEL

A numerical model to simulate FRP-strengthened concrete beam is formulated by using the SEM [10, 11]. The model is assumed to be one-dimensional. It consists of spectral concrete beam elements, spectral FRP-concrete beam elements and bonded-PZT FRP-concrete beam elements.

The governing equations for each one of the three element types were derived using Hamilton's principle. The general expression of these equations for any of the three element types takes the following form

$$\delta u_0 : I_0 \ddot{u}_0 - I_1 \ddot{\phi} + I_{0FRP} \ddot{s} - A_{11} u_{0,xx} + B_{11} \phi_{,xx} - A_{FRP} s_{,xx} = 0 \quad (1)$$

$$\delta w : I_0 \ddot{w} - A_{22} w_{,xx} + A_{22} \phi_{,x} = 0$$

$$\delta \phi : I_2 \ddot{\phi} - I_1 \ddot{u}_0 - I_{1FRP} \ddot{s} + B_{11} u_{0,xx} - D_{11} \phi_{,xx} - A_{22} w_{,x} + A_{22} \phi + B_{FRP} s_{,xx} = 0$$

$$\delta s : I_{0FRP} \ddot{s} + I_{0FRP} u_0 - I_{1FRP} \ddot{\phi} - A_{FRP} s_{,xx} - A_{FRP} u_{0,xx} + B_{FRP} \phi_{,xx} + \frac{G_{AD} s b_{AD}}{e_{AD}} = 0$$

where u_0 , w , ϕ and s are the mid-plane axial displacement, the transverse displacement, the rotation of the beam cross-section about the Y -axis and the slip of the FRP-concrete interface, respectively and G_{AD} , b_{AD} and e_{AD} denote the shear modulus the width and thickness of adhesive layer between FRP plate and RC beam.

The coefficients A_{11} , B_{11} , D_{11} , A_{22} , A_{FRP} and B_{FRP} are the stiffness coefficients related to material properties of concrete, FRP and PZT, depending on the type of element simulated

[12]. The same occurs with the coefficients, I_0 , I_1 and I_2 , related to inertial terms.

For spectral element formulation, the displacement field $\{u\} = \{u_0(x, t), w(x, t), \phi(x, t), s(x, t)\}$ can be written as

$$\{u\} = \sum_{n=1}^N \{\hat{u}(x, \omega_n)\} e^{-j\omega_n t} = \sum_{n=1}^N \left(\sum_{m=1}^M \{\hat{u}^*\}_{mn} e^{-jk_{mn}x} \right) e^{-j\omega_n t} \quad (2)$$

where ω_n is the n -th circular frequency, N is the number of sampling points while implementing Fast Fourier Transform (FFT) algorithm and $\hat{u}(x, \omega_n)$ represents the spectral amplitude vector corresponding to the generic displacement vector as a function of (x, ω_n) , k_{mn} denotes the m -th wave number related to n -th frequency ω_n . A Fourier expansion of $\hat{u}(x, \omega_n)$ has been also carried out in the longitudinal direction where $\{\hat{u}^*\}_{mn} = (\hat{u}_0, \hat{w}, \hat{\phi}, \hat{s})_{mn}$ represents the wave coefficient vector associated with the m -th mode of wave and for each frequency ω_n .

Replacing the assumed solution of the field variables in the governing equations (1) and solving for nontrivial solutions of the resulting equations, a characteristic equation is obtained whose solution gives eight eigenvalues (k_{mn} where $m=1, \dots, 8$) and eigenvectors ($\{\hat{u}^*\}$) for each frequency ω_n . In this way, from Eq. (2), the spectral amplitude vector, $\hat{u}(x, \omega_n)$, is obtained. With this method, each element can exactly represent the structural dynamics rather than approximate it as with FEM. If there are not discontinuities, one element can be used to model an entire section of the beam, reducing greatly, in this way, the computational cost of the problem. If progression of cracks of a concrete beam wants to be represented, several elements should be used with the purpose of capturing the discontinuities provided by the cracks.

The impedance signature (or admittance Y) at each sensor is obtained as follows [13]

$$Y(\omega) = j\omega \frac{b_{PZT} l_{PZT}}{e_{PZT}} \left(\bar{\epsilon}_{33}^T - \frac{Z_s(\omega)}{Z_s(\omega) + Z_a(\omega)} d_{31}^2 \bar{Y}_{11}^E \right) \quad (3)$$

where d_{31} is the piezoelectric strain constant between z and x directions at zero stress, $\bar{\epsilon}_{33}^T = \epsilon_{33}^T (1 - \delta j)$ is the complex electric permittivity of the PZT at constant stress, δ is the dielectric loss factor, j is the imaginary unit and l_{PZT} is the length of the PZT sensor; Furthermore, $Z_a(\omega)$ and $Z_s(\omega)$ represent the mechanical impedances of the PZT and the host structure. The first one depends mainly on the PZT properties and the second one is computed from the axial displacement computed from the spectral model [17].

3 DAMAGE IDENTIFICATION PROCEDURE

A model updating procedure is implemented for damage identification. For this methodology, the objective functions are formulated using impedances. Specifically, for each sensor k , an objective function to evaluate the agreement between experimental and numerical impedances is defined based on the cross-correlation coefficient (CC), which is usually employed as indicator in the impedance method, as follows

$$F_k = 1 - \frac{(\{1-CC\}_{num}^T \{1-CC\}_{exp})^2}{(\{1-CC\}_{num}^T \{1-CC\}_{num})(\{1-CC\}_{exp}^T \{1-CC\}_{exp})} \quad (4)$$

where the subscripts *num* and *exp* are used for the computed and measured responses, respectively. This function, applied to each *k*th sensor, has the advantage that its value is between 0 and 1. An index equal to one means no correlation between the sets of experimental and numerical impedances, while a value equal to zero indicates a perfect correlation between the updated numerical model and the experimental results. CC indicator is defined as follows

$$CC = \frac{1}{n} \sum_{i=1}^n \frac{\{Z_0(\omega_i) - \bar{Z}_0\} \{Z_1(\omega_i) - \bar{Z}_1\}}{\sigma_{Z_0} \sigma_{Z_1}} \quad (5)$$

where $Z_0(\omega_i)$ is the impedance of the PZT measured at a previous stage, which might agree with the healthy condition of the structure, and $Z_1(\omega_i)$ is the corresponding value at a subsequent stage, which might agree with a post-damage stage, at the *i*th frequency point; *n* is the number of frequency points; $\bar{Z}_0(\omega_i)$ and $\bar{Z}_1(\omega_i)$ are the mean values of the two data sets, $Z_0(\omega_i)$ and $Z_1(\omega_i)$, respectively, and σ_{Z_0} and σ_{Z_1} are the standard deviations of the two corresponding data sets, $Z_0(\omega_i)$ and $Z_1(\omega_i)$.

In the damage identification procedure, the damage at FRP-RC interface has been chosen as parameter to be updated. This damage is defined as follows

$$d_e = 1 - \frac{(G_{AD})_d^e}{(G_{AD})^e} \quad (6)$$

where $(G_{AD})^e$ and $(G_{AD})_d^e$ are the adhesive stiffnesses for element *e* before and after debonding damage, respectively. The case of $d_e=0$ indicates the intact state while $d_e=1$ means that the element *e* has debonded completely.

4 RESULTS

In order to validate the feasibility of the proposed spectral approach and check the ability of the proposed model updating method as a damage identification procedure, some experimental tests were performed on a concrete block strengthened with an FRP strip (Fig. 1). Three PZT sensors were bonded to the external face of the FRP reinforcement. The impedances were measured for the three sensors considering two different stages of the block: a) Stage A: Healthy stage; b) Stage B: A 2.4 cm length hole-type damage was introduced at the FRP-concrete interface at a distance of 7 cm from the left end of the concrete block (Fig.2).

The impedance signals in a wide frequency range (10-100 kHz) were divided into nine subranges with 10 kHz each. Then, the CC vector defining the objective function in Eq.(4) was constructed with nine CC values calculated in nine sub-frequency ranges.

To apply the proposed damage detection strategy, a very simple spectral numerical model was implemented originally for the specimen. The model consists of 7 spectral elements (E1 to E7) and 8 nodes (N1 to N8) whose coordinates were suitably chosen to be coincident with

the sensor locations and the damaged area (Fig. 3). The number of spectral elements used in the tested specimen to capture the high frequency impedance response is very low compared to the conventional finite element method.

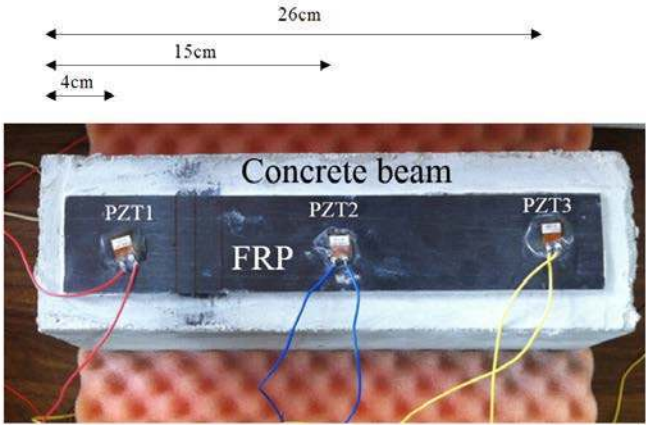


Figure 1: Tested specimen.

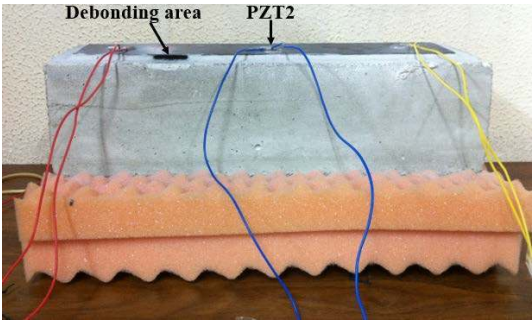


Figure 2: Location of the debonding area.

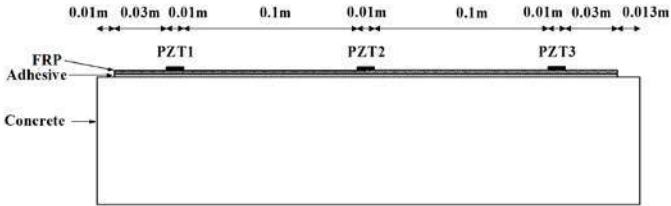


Figure 3: Spectral element mesh.

Three different scenarios were considered, unnoisy, 1% and 5% of noise, i.e., the lab data obtained from sensors were contaminated with artificial noise of severity 1% and 5%.

Fig. 4 shows the identification results for the three scenarios. Predictions with 1% noise are good and are very similar to the unnoisy case. Furthermore, Fig. 4 confirms that the damage prediction is not so influenced by the effect of 5% noise.

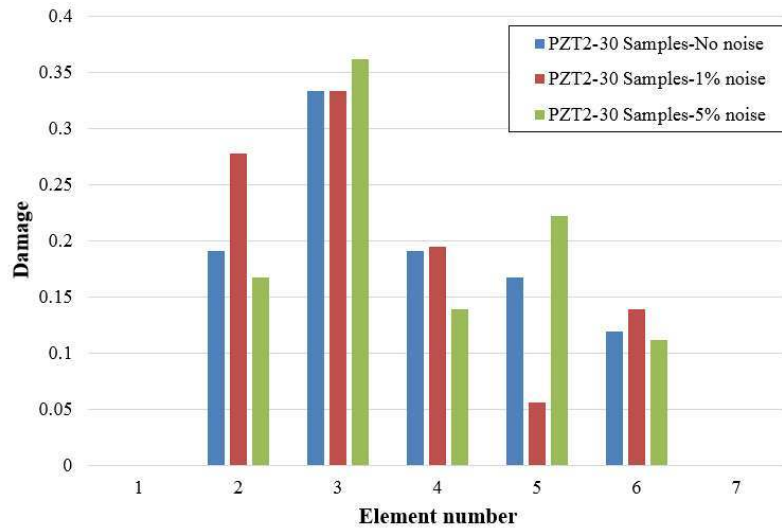


Figure 4: Damage predictions.

5 CONCLUSIONS

A methodology to diagnose damage due to intermediate interfacial debonding in FRP flexural strengthened RC beams has been proposed. The approach is based on a PZT impedance actuator-sensor. These kinds of transducers works in the high frequency range which makes them especially suitable to detect minor debondings. The adopted strategy is based on a model updating procedure and has been carried out with a proposed model of the bonded-PZT FRP strengthened beam based on a one-dimensional simplified spectral element method.

An experimental study was performed to validate the proposed scheme. Successful predictions have demonstrated the importance of the proposed methodology.

ACKNOWLEDGEMENTS

The writers acknowledge the support for the work reported in this paper from the Spanish Ministry of Economy and Competitiveness (project BIA2013-46944-C2-1-P).

REFERENCES

- [1] JG Teng, JF Chen, ST Smith, L Lam, “*FRP Strengthened RC Structures*”, first ed. John Wiley and Sons, West Sussex (2002).
- [2] LC Bank, “*Composites for construction: Structural design with FRP materials*”, first ed. John Wiley and Sons (2006).
- [3] P Balaguru, A Nanni, J Giancaspro, “*FRP Composites for Reinforced and Prestressed Concrete Structures. A guide to fundamentals and design for repair and retrofit*”, first ed. Taylor and Francis, New York and London (2009).
- [4] A Rahimi, A Hutchinson, Concrete Beams Strengthened with Externally Bonded FRP Plates. *Journal of Composites for Construction*, **5**, 44-56, 2001.

- [5] L Ascione, L Feo, Modeling of composite/concrete interface of RC beams strengthened with composite laminates. *Composites. Part B: Engineering*, **31**, 535-540, 2000.
- [6] N Pesic, K Pilakoutas, Concrete beams with externally bonded flexural FRP-reinforcement: analytical investigation of debonding failure. *Composites. Part B: Engineering*, **34**, 327-338, 2003.
- [7] ST Liu, DJ Oehlers, R Seracino, Study of Intermediate Crack Debonding in Adhesively Plated Beams. *Journal of Composites in Construction*, **11**, 175–183, 2007.
- [8] GM Chen, JG Teng, JF Chen, Finite-Element Modeling of Intermediate Crack Debonding in FRP-Plated RC Beams. *Journal of Composites in Construction*, **15**, 339–353, 2011
- [9] R Perera, E Sevillano, A Arteaga, A De Diego, Identification of intermediate debonding damage in FRP-plated RC beams based on multi-objective particle swarm optimization without updated baseline model. *Composites. Part B: Engineering*, **62**, 205–217, 2014.
- [10] JF Doyle JF, “*Wave propagation in structures*”, Springer (1997).
- [11] S Gopalakrishnan, A Ghakraborty, D Roy Mahapatra, “*Spectral finite element method*”, first ed. Springer, London (2008).
- [12] R Perera, D Bueso-Inchausti, A unified approach for the static and dynamic analyses of intermediate debonding in FRP-strengthened reinforced concrete beams. *Composites Structures*, **92**, 2728-37, 2010.
- [13] C Liang, FP Sun, CA Rogers, Coupled electro-mechanical analysis of adaptive material system-determination of the actuator power consumption and system energy transfer. *Journal of Intelligent Material Systems and Structures*, **5**, 12-20, 1994..